Journal of Computational and Applied Mathematics 362 (2019) 614–625

Contents lists available at ScienceDirect

Journal of Computational and Applied Mathematics

journal homepage: www.elsevier.com/locate/cam

A weak Galerkin finite element method for the Navier–Stokes equations[☆]

Xiaozhe Hu[a,*], Lin Mu[b], Xiu Ye[c]

[a] Department of Mathematics, Tufts University, Medford, MA 02155, USA
[b] Computer Science and Mathematics Division, Oak Ridge National Laboratory, Oak Ridge, TN, 37831, USA
[c] Department of Mathematics, University of Arkansas at Little Rock, Little Rock, AR, USA

ARTICLE INFO

Article history:
Received 9 December 2017
Received in revised form 6 June 2018

Keywords:
Weak Galerkin
Finite element methods
The Navier–Stokes equations
Polyhedral meshes

ABSTRACT

This paper introduces a weak Galerkin (WG) finite element method for the Navier–Stokes equations in the primal velocity–pressure formulation. Optimal-order error estimates are established for the corresponding numerical approximations. It must be emphasized that the WG finite element method is designed on finite element partitions consisting of arbitrary shape of polygons or polyhedra which are shape regular. Numerical experiments are presented to support the theoretical results.

1. Introduction

In this paper, we develop a weak Galerkin (WG) finite element method for the Navier–Stokes (NS) equations which seeks velocity $\boldsymbol{u}$ and pressure p satisfying

$$-\mu\Delta\boldsymbol{u}+\boldsymbol{u}\cdot\nabla\boldsymbol{u}+\nabla p=\mathbf{f}\quad\text{in }\Omega, \tag{1}$$

$$\nabla\cdot\boldsymbol{u}=0\quad\text{in }\Omega, \tag{2}$$

$$\boldsymbol{u}=0\quad\text{on }\partial\Omega, \tag{3}$$

where Ω is a polygonal or polyhedral domain in $\mathbb{R}^d$ $(d=2,3)$ and μ is the viscosity of the fluid. The weak formulation of the primal velocity–pressure NS equations (1)–(3) seeks $\boldsymbol{u}\in[H_0^1(\Omega)]^d$ and $p\in L_0^2(\Omega)$ such that, for all $\boldsymbol{v}\in[H_0^1(\Omega)]^d$ and $q\in L_0^2(\Omega)$,

$$\mu(\nabla\boldsymbol{u},\nabla\boldsymbol{v})+(\boldsymbol{u}\cdot\nabla\boldsymbol{u},\boldsymbol{v})-(\nabla\cdot\boldsymbol{v},p)=(\mathbf{f},\boldsymbol{v}), \tag{4}$$

$$(\nabla\cdot\boldsymbol{u},q)=0. \tag{5}$$

Here $[H_0^1(\Omega)]^d=\{\boldsymbol{u}\in[H^1(\Omega)]^d:\boldsymbol{u}|_{\partial\Omega}=0\}$ and $L_0^2(\Omega)=\{p\in L^2(\Omega):\int_\Omega p=0\}$ with $[H^1(\Omega)]^d$ being the space of square integrable vector-valued functions whose first derivatives are also square integrable and $L^2(\Omega)$ being the space of square

☆ The work of X. Hu was supported in part by National Science Foundation Grant DMS-1620063. The research of L. Mu is based upon work supported in part by the U.S. Department of Energy, Office of Science, Office of Advanced Scientific Computing Research, Applied Mathematics program under award number ERKJE45; and by the Laboratory Directed Research and Development program at the Oak Ridge National Laboratory, which is operated by UT-Battelle, LLC., for the U.S. Department of Energy under Contract DE-AC05-00OR22725. The work of X. Ye was supported in part by National Science Foundation Grant DMS-1620016.

* Corresponding author.
E-mail addresses: Xiaozhe.Hu@tufts.edu (X. Hu), mul1@ornl.gov (L. Mu), xxye@ualr.edu (X. Ye).

https://doi.org/10.1016/j.cam.2018.08.022
0377-0427/

integrable functions. Based on the fact that $\nabla \cdot \boldsymbol{u} = 0$, the weak formulation (4) and (5) can be written as the follows,

$$\mu(\nabla \boldsymbol{u}, \nabla \boldsymbol{v}) + \frac{1}{2}((\boldsymbol{u} \cdot \nabla \boldsymbol{u}, \boldsymbol{v}) - (\boldsymbol{u} \cdot \nabla \boldsymbol{v}, \boldsymbol{u})) - (\nabla \cdot \boldsymbol{v}, p) = (\mathbf{f}, \boldsymbol{v}), \tag{6}$$

$$(\nabla \cdot \boldsymbol{u}, q) = 0, \tag{7}$$

where $\frac{1}{2}((\boldsymbol{u} \cdot \nabla \boldsymbol{u}, \boldsymbol{v}) - (\boldsymbol{u} \cdot \nabla \boldsymbol{v}, \boldsymbol{u}))$ is skew symmetric. This is a classical stabilization technique for solving Navier–Stokes equations, c.f. [1].

Due to the importance of the NS equations, the developments of robust numerical schemes for the NS equations have drawn great attentions for the last several decades. The continuous finite element methods for the NS equations usually require a pair of finite element spaces that is conforming in $[H^1]^d \times L^2$ and satisfies the *inf–sup* condition [2,3]. Many schemes have been proposed based on different choices of the finite element pairs and we refer the readers to [4,5] for more details. On the other hand, due to the convection dominance and incompressibility of the NS equations, discontinuous Galerkin (DG) finite element methods [6–8] seem to be more suitable and become more and more popular, see [9–14] and references therein.

Most of those finite element methods are designed for triangular or rectangular meshes in 2D or tetrahedrons or hexahedrons in 3D. In recent years, considerable attention has been paid to the development of the finite element methods using polygonal and polyhedral meshes. Many numerical schemes have been developed on general polytopal meshes [15–19] for second order elliptic problems and [20–22] for the Navier–Stokes equations. In this work, we introduce a weak Galerkin finite element method for solving the incompressible NS equations on polytopal meshes. The WG methods, first proposed and analyzed by Wang and Ye [23] recently, provide a general finite element technique for solving partial differential equations. In general, WG methods approximate the differential operators in PDEs by their weak forms as distributions for generalized functions. The WG methods have been successively applied to the second order elliptic equations in the primal form [23], and mixed form [24] for general finite element partitions of arbitrary shape [25]. Recent work on WG methods reveal that the concept of discrete weak derivatives offers a new paradigm for numerically solving PDEs and the WG methods often provide robust and stable discertizations for various problems. For examples, stable discretization for Stokes equations [26,27], stable discretization for the Brinkman equations [28], locking-free scheme for the linear elasticity problems in the primal formulation [29], and the poroelasticity [30].

In this work, we develop weak Galerkin finite element method for solving the NS equations on polytopal meshes. The WG formulation for the NS equations can be derived from the weak form (6)–(7) by simply replacing the strong derivatives by weakly defined derivatives and adding a parameter free stabilizer $s(\cdot, \cdot)$ as follows,

$$\mu(\nabla_w \boldsymbol{u}, \nabla_w \boldsymbol{v}) + \frac{1}{2}\left[(\boldsymbol{u} \cdot \nabla_w \boldsymbol{u}, \boldsymbol{v}) - (\boldsymbol{u} \cdot \nabla_w \boldsymbol{v}, \boldsymbol{u})\right] - (\nabla_w \cdot \boldsymbol{v}, p) + s(\boldsymbol{u}_h, \boldsymbol{v}) = (\mathbf{f}, \boldsymbol{v}),$$

$$(\nabla_w \cdot \boldsymbol{u}, q) = 0.$$

Detailed definitions of those weak derivatives and stabilizer will be discussed later. Our approach extends the WG scheme for the Stokes equations [26,27] and retains the advantages of the WG methods. Our WG scheme allows the flexibility of the choices of the polynomials and also works on general polyhedral meshes. We show that, under standard assumptions, the WG scheme provides an approximate velocity and pressure converging with the optimal order in an energy norm defined on the WG spaces. Numerical results demonstrate the effectiveness of the proposed WG scheme, especially on general polyhedral meshes.

The rest of the paper is organized as follows. In Section 2, we introduce the weak derivatives and our WG formulation for the NS equations. In Section 3, we study the existence and uniqueness of the WG solutions. We derive the error estimate for the WG approximation in Section 4. Optimal-order convergence is proved under certain regularity assumption. Finally, we present some numerical experiments to demonstrate the effectiveness of the WG approximation in Section 5 .

2. A weak Galerkin finite element scheme

In this section, we introduce the WG scheme. Let $\mathcal{T}_h$ be a partition of the domain Ω consisting of polygons in two dimensions or polyhedra in three dimensions satisfying a set of conditions specified in [24]. Denote by $\mathcal{E}_h$ the set of all edges or flat faces in $\mathcal{T}_h$ and let $\mathcal{E}_h^0 = \mathcal{E}_h \setminus \partial\Omega$ be the set of all interior edges or flat faces. For every element $T \in \mathcal{T}_h$, we denote by h_T its diameter and define mesh size $h = \max_{T \in \mathcal{T}_h} h_T$ for $\mathcal{T}_h$. In addition, throughout our paper, we use C to denote generic constant that is independent of mesh size h.

On the mesh $\mathcal{T}_h$, we define WG finite element space V_h^0 for the velocity as follows,

$$V_h^0 := \{\boldsymbol{v} = \{\boldsymbol{v}_0, \boldsymbol{v}_b\} \in V_h, \boldsymbol{v}_b = 0 \text{ on } \partial\Omega\},$$

where

$$V_h = \left\{\boldsymbol{v} = \{\boldsymbol{v}_0, \boldsymbol{v}_b\} : \ \boldsymbol{v}_0|_T \in [P_k(T)]^d, \boldsymbol{v}_b|_e \in [P_k(e)]^d, \ e \subset \partial T, \ \forall T \in \mathcal{T}_h\right\}.$$

Here P_k denotes the space of polynomials of degree no more than k. We would like to emphasize that there is only single value $\boldsymbol{v}_b$ defined on each edge $e \in \mathcal{E}_h$. For the pressure, we define the following finite element space,

$$W_h = \left\{q \in L_0^2(\Omega), \ q|_T \in P_{k-1}(T), \ \forall T \in \mathcal{T}_h\right\}.$$

Remark 2.1. Other choices of WG finite element space can also be used without changing our analysis. For example, we can use $\boldsymbol{v}_0|_T \in [P_k(T)]^d$ and $\boldsymbol{v}_b|_e \in [P_{k-1}(e)]^d$ as suggested in [26] and [31], which leads to less degrees of freedoms than the choice we presented above. Our analysis applies to this choice of the WG finite element space as well.

We define the weak derivatives that are used to derive the WG scheme. For $\boldsymbol{v} \in V_h$ and $T \in \mathcal{T}_h$, we define weak gradient $\nabla_w \boldsymbol{v} \in [P_{k-1}(T)]^{d\times d}$ as the unique polynomial satisfying the following equation

$$(\nabla_w \boldsymbol{v}, \tau)_T = -(\boldsymbol{v}_0, \nabla\cdot\tau)_T + \langle \boldsymbol{v}_b, \tau\cdot\mathbf{n}\rangle_{\partial T}, \quad \forall \tau \in [P_{k-1}(T)]^{d\times d}, \tag{8}$$

and define weak divergence $\nabla_w \cdot \boldsymbol{v} \in P_{k-1}(T)$ as the unique polynomial satisfying

$$(\nabla_w \cdot \boldsymbol{v}, q)_T = -(\boldsymbol{v}_0, \nabla q)_T + \langle \boldsymbol{v}_b, q\mathbf{n}\rangle_{\partial T}, \quad \forall q \in P_{k-1}(T), \tag{9}$$

where $(\cdot,\cdot)_T = (\cdot,\cdot)_{L^2(T)}$.

Next, we define the following broken inner product,

$$(v, w)_{\mathcal{T}_h} = \sum_{T\in\mathcal{T}_h} (v, w)_T = \sum_{T\in\mathcal{T}_h} \int_T vw\, \mathrm{d}\boldsymbol{x},$$
$$\langle v, w\rangle_{\partial\mathcal{T}_h} = \sum_{T\in\mathcal{T}_h} \langle v, w\rangle_{\partial T} = \sum_{T\in\mathcal{T}_h} \int_{\partial T} vw\, \mathrm{d}s,$$

and introduce some bilinear forms as follows,

$$\begin{aligned}
s(\boldsymbol{v},\ \boldsymbol{w}) &= \sum_{T\in\mathcal{T}_h} h_T^{-1} \langle \boldsymbol{v}_0 - \boldsymbol{v}_b,\ \ \boldsymbol{w}_0 - \boldsymbol{w}_b\rangle_{\partial T},\\
a_w(\boldsymbol{v},\ \boldsymbol{w}) &= \mu(\nabla_w \boldsymbol{v},\ \nabla_w \boldsymbol{w})_{\mathcal{T}_h} + \mu s(\boldsymbol{v}, \boldsymbol{w}),\\
b_w(\boldsymbol{v},\ q) &= (\nabla_w\cdot \boldsymbol{v},\ q)_{\mathcal{T}_h},\\
a_{sk}(\boldsymbol{v}, \boldsymbol{w}, \boldsymbol{\sigma}) &= \frac{1}{2}\left[(\boldsymbol{v}\cdot\nabla \boldsymbol{w}, \boldsymbol{\sigma})_{\mathcal{T}_h} - (\boldsymbol{v}\cdot\nabla\boldsymbol{\sigma}, \boldsymbol{w})_{\mathcal{T}_h}\right]\\
a_{sk,w}(\boldsymbol{v}, \boldsymbol{w}, \boldsymbol{\sigma}) &= \frac{1}{2}\left[(\boldsymbol{v}\cdot\nabla_w \boldsymbol{w}, \boldsymbol{\sigma})_{\mathcal{T}_h} - (\boldsymbol{v}\cdot\nabla_w\boldsymbol{\sigma}, \boldsymbol{w})_{\mathcal{T}_h}\right].
\end{aligned}$$

We are now in a position to describe the WG finite element scheme for the NS equations (1)–(3).

Weak Galerkin Scheme 1. Find $\boldsymbol{u}_h \in V_h^0$ and $p_h \in W_h$, such that

$$a_w(\boldsymbol{u}_h,\ \boldsymbol{v}) + a_{sk,w}(\boldsymbol{u}_h, \boldsymbol{u}_h, \boldsymbol{v}) - b_w(\boldsymbol{v},\ p_h) = (f,\ \boldsymbol{v}), \quad \forall \boldsymbol{v}\in V_h^0, \tag{10}$$

$$b_w(\boldsymbol{u}_h,\ q) = 0, \qquad \forall q \in W_h. \tag{11}$$

3. Existence and uniqueness of the WG solution

In this section, we discuss the well-posedness of the WG scheme 1. The main theoretical tool we use is the Leray–Schauder fixed point theorem. First, we introduce the following norm for the WG finite element space V_h^0,

$$|||\boldsymbol{v}|||^2 = \sum_{T\in\mathcal{T}_h} \|\nabla_w \boldsymbol{v}\|_T^2 + \sum_{T\in\mathcal{T}_h} h_T^{-1}\|\boldsymbol{v}_0 - \boldsymbol{v}_b\|_{\partial T}^2. \tag{12}$$

Next, we present some lemmas that are used in our analysis. Let $\mathbb{Q}_h$ and $\mathbf{Q}_h$ be two local L^2 projections onto $P_{k-1}(T)$, and $[P_{k-1}(T)]^{d\times d}$, respectively. The L^2 projection Q_h of $\boldsymbol{u}$ to the WG finite element space V_h is defined by $Q_h\boldsymbol{u} = \{Q_0\boldsymbol{u}, Q_b\boldsymbol{u}\}$ with Q_0 being the L^2 projection onto $[P_k(T)]^d$ and Q_b being the L^2 projection onto $[P_k(e)]^d$. The following three lemmas have been proved in [26].

Lemma 3.1. *For any $\boldsymbol{v}, \boldsymbol{w} \in V_h$, we have*

$$|a_w(\boldsymbol{v}, \boldsymbol{w})| \le \mu |||\boldsymbol{v}|||\,|||\boldsymbol{w}|||, \tag{13}$$

$$a_w(\boldsymbol{v}, \boldsymbol{v}) = \mu|||\boldsymbol{v}|||^2. \tag{14}$$

Lemma 3.2. *The projection operators Q_h, $\mathbf{Q}_h$, and $\mathbb{Q}_h$ satisfy the following commutative properties*

$$\nabla_w(Q_h\boldsymbol{v}) = \mathbf{Q}_h(\nabla\boldsymbol{v}), \qquad \forall \boldsymbol{v}\in[H^1(\Omega)]^d, \tag{15}$$

$$\nabla_w\cdot(Q_h\boldsymbol{v}) = \mathbb{Q}_h(\nabla\cdot\boldsymbol{v}), \qquad \forall \boldsymbol{v}\in H(\mathrm{div},\Omega), \tag{16}$$

where $H(\mathrm{div},\Omega)$ is the space of square integrable vector-valued functions whose divergence is also square integrable.

Lemma 3.3. *There exists a positive constant β independent of h such that*

$$\sup_{\boldsymbol{v}\in V_h^0}\frac{b_w(\boldsymbol{v},\rho)}{|||\boldsymbol{v}|||}\geq \beta\|\rho\|,\quad \forall\,\rho\in W_h. \tag{17}$$

The following inequality can be verified easily (see [32] for details),

$$s(\boldsymbol{v},\boldsymbol{v})=\sum_{T\in\mathcal{T}_h}h_T^{-1}\|\boldsymbol{v}_0-\boldsymbol{v}_b\|_{\partial T}^2\geq\frac{1}{2}\sum_{e\in\mathcal{E}_h}h_e^{-1}\|[\boldsymbol{v}_0]\|_e^2. \tag{18}$$

It has been proved in [31] that, for $\boldsymbol{v}=\{\boldsymbol{v}_0,\boldsymbol{v}_b\}\in V_h$,

$$\sum_{T\in\mathcal{T}_h}\|\nabla\boldsymbol{v}_0\|_T^2\leq C|||\boldsymbol{v}|||^2. \tag{19}$$

Define another norm $|||\boldsymbol{v}|||_1$ on V_h for $\boldsymbol{v}=\{\boldsymbol{v}_0,\boldsymbol{v}_b\}$ as follows,

$$|||\boldsymbol{v}|||_1^2=\sum_{T\in\mathcal{T}_h}\|\nabla\boldsymbol{v}_0\|_T^2+\sum_{e\in\mathcal{E}_h}h_e^{-1}\|[\boldsymbol{v}_0]\|_e^2. \tag{20}$$

Then, it follows from (18) and (19) that,

$$|||\boldsymbol{v}|||_1\leq C|||\boldsymbol{v}|||,\quad \forall\,\boldsymbol{v}\in V_h. \tag{21}$$

The following lemma has been proved in [33], which gives a upper bound of the trilinear form $a_{sk}(\cdot,\cdot,\cdot)$ by the $|||\cdot|||_1$ norm.

Lemma 3.4. *Let $\boldsymbol{\sigma},\boldsymbol{v},\boldsymbol{w}\in V_h$ and $|||\cdot|||_1$ be defined in (20). Then we have*

$$\|\boldsymbol{w}\|_{L^4(\Omega)}\leq C|||\boldsymbol{w}|||_1, \tag{22}$$

$$a_{sk}(\boldsymbol{\sigma},\boldsymbol{v},\boldsymbol{w})\leq C|||\boldsymbol{\sigma}|||_1|||\boldsymbol{v}|||_1|||\boldsymbol{w}|||_1. \tag{23}$$

Finally, we present the following lemma which gives an upper bound of the trilinear form $a_{sk,w}(\cdot,\cdot,\cdot)$ by the $|||\cdot|||$ norm.

Lemma 3.5. *For $\boldsymbol{\sigma}=\{\boldsymbol{\sigma}_0,\boldsymbol{\sigma}_b\}$, $\boldsymbol{v}=\{\boldsymbol{v}_0,\boldsymbol{v}_b\}$, and $\boldsymbol{w}=\{\boldsymbol{w}_0,\boldsymbol{w}_b\}$ in V_h, we have*

$$|a_{sk,w}(\boldsymbol{\sigma},\boldsymbol{v},\boldsymbol{w})|\leq\mathcal{N}_h|||\boldsymbol{\sigma}|||\,|||\boldsymbol{v}|||\,|||\boldsymbol{w}|||, \tag{24}$$

where $\mathcal{N}_h$ is a constant independent of h.

Proof. Eqs. (21) and (22) imply

$$\begin{aligned}|a_{sk,w}(\boldsymbol{\sigma},\boldsymbol{v},\boldsymbol{w})| &\leq \frac{1}{2}\sum_{T\in\mathcal{T}_h}\|\boldsymbol{\sigma}_0\|_{L^4(T)}(\|\boldsymbol{w}_0\|_{L^4(T)}\|\nabla_w\boldsymbol{v}\|_T+\|\boldsymbol{v}_0\|_{L^4(T)}\|\nabla_w\boldsymbol{w}\|_T)\\ &\leq \frac{1}{2}\|\boldsymbol{\sigma}_0\|_{L^4(\Omega)}(\|\boldsymbol{w}_0\|_{L^4(\Omega)}|||\boldsymbol{v}|||+\|\boldsymbol{v}_0\|_{L^4(\Omega)}|||\boldsymbol{w}|||)\\ &\leq C|||\boldsymbol{\sigma}|||_1(|||\boldsymbol{w}|||_1|||\boldsymbol{v}|||+|||\boldsymbol{v}|||_1|||\boldsymbol{w}|||)\\ &\leq \mathcal{N}_h|||\boldsymbol{\sigma}|||\,|||\boldsymbol{v}|||\,|||\boldsymbol{w}|||.\end{aligned}$$

Here the constant $\mathcal{N}_h$ depends on the constants in (21) and (22). Therefore, it is independent of h as well. This completes the proof. □

With all these preparations, now we are ready to apply the Leray–Schauder fixed point theorem to the WG scheme (10) and (11) and show the existence and uniqueness of the solution. To this end, we introduce a discrete divergent free subspace D_h of V_h as follows:

$$D_h=\{\boldsymbol{v}\in V_h:\ \nabla_w\cdot\boldsymbol{v}_h=0\}.$$

Then the WG formulation (10) and (11) can be reformulated as seeking $\boldsymbol{u}_h\in D_h$ such that

$$a_w(\boldsymbol{u}_h,\boldsymbol{v})+a_{sk,w}(\boldsymbol{u}_h,\boldsymbol{u}_h,\boldsymbol{v})=(\mathbf{f},\boldsymbol{v}),\quad\forall\,\boldsymbol{v}\in D_h. \tag{25}$$

Let $F:D_h\to D_h$ be a nonlinear map so that for each $\boldsymbol{w}_h\in D_h$, $\tilde{\boldsymbol{u}}_h:=F(\boldsymbol{w}_h)\in D_h$ is given as the solution of the following linear problem:

$$a_w(\tilde{\boldsymbol{u}}_h,\boldsymbol{v})+a_{sk,w}(\boldsymbol{w}_h,\tilde{\boldsymbol{u}}_h,\boldsymbol{v})=(\mathbf{f},\boldsymbol{v}),\quad\forall\,\boldsymbol{v}\in D_h. \tag{26}$$

The map F is clearly continuous and, therefore, compact in the finite dimensional space D_h. If $\lambda > 0$ and $\boldsymbol{w}_h$ satisfies $F(\boldsymbol{w}_h) = \lambda \boldsymbol{w}_h$, then from (26), we have

$$\lambda\, a_w(\boldsymbol{w}_h, \boldsymbol{v}) + \lambda\, a_{sk,w}(\boldsymbol{w}_h, \boldsymbol{w}_h, \boldsymbol{v}) = (\mathbf{f}, \boldsymbol{v}), \quad \forall\, \boldsymbol{v} \in D_h. \tag{27}$$

By choosing $\boldsymbol{v} = \boldsymbol{w}_h$ in (27), we obtain that

$$\lambda \left(a_w(\boldsymbol{w}_h, \boldsymbol{w}_h) + a_{sk,w}(\boldsymbol{w}_h, \boldsymbol{w}_h, \boldsymbol{w}_h)\right) = (\mathbf{f}, \boldsymbol{w}_h), \quad \forall\, \boldsymbol{v} \in D_h.$$

It now follows from (14) that

$$\lambda\, \mu\, |||\boldsymbol{w}_h|||^2 \leq |(\mathbf{f}, \boldsymbol{w}_h)|. \tag{28}$$

By introducing a mesh-dependent norm

$$\|\mathbf{f}\|_{*,h} = \sup_{\boldsymbol{v} \in D_h} \frac{(\mathbf{f}, \boldsymbol{v})}{|||\boldsymbol{v}|||}, \tag{29}$$

we have,

$$\lambda \mu |||\boldsymbol{w}_h|||^2 \leq \|\mathbf{f}\|_{*,h} |||\boldsymbol{w}_h|||.$$

Therefore,

$$\lambda \leq \frac{\|\mathbf{f}\|_{*,h}}{\mu |||\boldsymbol{w}_h|||}.$$

Thus, $\lambda < 1$ holds true for any $\boldsymbol{w}_h$ being on the boundary of the ball in D_h centered at the origin with radius $\rho > \frac{\|\mathbf{f}\|_{*,h}}{\mu}$. Consequently, the Leray–Schauder fixed point theorem implies that the nonlinear map F defined by (26) has a fixed point $\boldsymbol{u}_h$ such that,

$$F(\boldsymbol{u}_h) = \boldsymbol{u}_h$$

in any ball centered at the origin with radius $\rho > \frac{\|\mathbf{f}\|_{*,h}}{\mu}$. This fixed point $\boldsymbol{u}_h$ also is a solution of the finite element scheme (25), which in turn provides a solution of the original WG scheme (10) and (11). These can be summarized in the following theorem.

Theorem 1. *The finite element discretization scheme* (25) *has at least one solution* $\boldsymbol{u}_h \in D_h$. *Moreover, all the solutions of* (25) *satisfy the following estimates:*

$$|||\boldsymbol{u}_h||| \leq \frac{\|\mathbf{f}\|_{*,h}}{\mu}. \tag{30}$$

Proof. Note that $\boldsymbol{u}_h \in D_h$ is a solution of (25) if and only if it is a fixed-point of the nonlinear map F. Since F has at least one fixed point in the ball of D_h centered at the origin with radius $\rho > \frac{\|\mathbf{f}\|_{*,h}}{\mu}$, then the finite element scheme (25) must have a solution and all the solutions must satisfy the estimate (30).

Let $\boldsymbol{u}_h$ be a solution of (25) and $\boldsymbol{v} = \boldsymbol{u}_h$ in (25). Since $a_{sk,w}(\boldsymbol{u}_h, \boldsymbol{u}_h, \boldsymbol{u}_h) = 0$, we have, $\mu |||\boldsymbol{u}_h|||^2 \leq \|\mathbf{f}\|_{*,h} |||\boldsymbol{u}_h|||$, which implies (30). □

Next, we show the uniqueness of the solution of (25). Let $\boldsymbol{u}_h$ and $\bar{\boldsymbol{u}}_h \in D_h$ be two solutions of the finite element scheme (25). Since both of them satisfy the nonlinear equation (25), let $\boldsymbol{\psi}_h = \boldsymbol{u}_h - \bar{\boldsymbol{u}}_h$, for all $\boldsymbol{v} \in D_h$, we have,

$$a_w(\boldsymbol{\psi}_h, \boldsymbol{v}) + a_{sk,w}(\boldsymbol{u}_h, \boldsymbol{u}_h, \boldsymbol{v}) - a_{sk,w}(\bar{\boldsymbol{u}}_h, \bar{\boldsymbol{u}}_h, \boldsymbol{v}) = 0.$$

Observe that,

$$a_{sk,w}(\boldsymbol{u}_h, \boldsymbol{u}_h, \boldsymbol{v}) - a_{sk,w}(\bar{\boldsymbol{u}}_h, \bar{\boldsymbol{u}}_h, \boldsymbol{v}) = a_{sk,w}(\boldsymbol{u}_h, \boldsymbol{\psi}_h, \boldsymbol{v}) + a_{sk,w}(\boldsymbol{\psi}_h, \bar{\boldsymbol{u}}_h, \boldsymbol{v}).$$

Thus, for any $\boldsymbol{v} \in D_h$, we have,

$$a_w(\boldsymbol{\psi}_h, \boldsymbol{v}) + a_{sk,w}(\boldsymbol{u}_h, \boldsymbol{\psi}_h, \boldsymbol{v}) = a_{sk,w}(\boldsymbol{\psi}_h, \bar{\boldsymbol{u}}_h, \boldsymbol{v}).$$

Letting $\boldsymbol{v} = \boldsymbol{\psi}_h$, from (14) and the fact that $a_{sk,w}(\boldsymbol{u}_h, \boldsymbol{\psi}_h, \boldsymbol{\psi}_h) = 0$, we obtain,

$$\mu |||\boldsymbol{\psi}_h|||^2 = \left|a_{sk,w}(\boldsymbol{\psi}_h, \bar{\boldsymbol{u}}_h, \boldsymbol{v})\right|$$

By Lemma 3.5, upper bound (24), we arrive at the following estimate,

$$\mu |||\boldsymbol{\psi}_h|||^2 \leq \mathcal{N}_h |||\bar{\boldsymbol{u}}_h|||\ |||\boldsymbol{\psi}_h|||^2. \tag{31}$$

Note that $\bar{\boldsymbol{u}}_h$ is a solution of (25), the estimate (30) in Theorem 1 is applicable, i.e., $|||\bar{\boldsymbol{u}}_h||| \leq \frac{\|\mathbf{f}\|_{*,h}}{\mu}$. Therefore, substituting back into the right-hand side of (31) yields

$$\mu|||\boldsymbol{\psi}_h|||^2 \leq \frac{\mathcal{N}_h\|\mathbf{f}\|_{*,h}}{\mu}|||\boldsymbol{\psi}_h|||^2. \tag{32}$$

which implies the uniqueness of the solutions under certain conditions. We summarize the result in the following theorem.

Theorem 2. *Let $\mathcal{N}_h$ be defined in (24). If $\frac{\mathcal{N}_h\|\mathbf{f}\|_{*,h}}{\mu^2} < 1$ holds true, then the WG finite element discretization scheme (25) has at most one solution in the discrete divergence-free subspace D_h.*

4. Error estimate

In this section, we discuss the convergence rate of the WG scheme. We first derive the error equations and then analyze the error estimates. For the sake of simplicity, we shall only present the results in two dimensions and comment that all the results can be extended to three dimensions naturally without much difficulties.

Let $\boldsymbol{u}_h = \{\boldsymbol{u}_0, \boldsymbol{u}_b\} \in V_h$ and $p_h \in W_h$ be the solution to the WG scheme (10)–(11). Let $\boldsymbol{u}$ and p be the exact solution of (1)–(3). Recall that $Q_h\boldsymbol{u} = \{Q_0\boldsymbol{u}, Q_b\boldsymbol{u}\}$. Similarly, the pressure p is projected onto W_h as $\mathbb{Q}_h p$. Then the errors $\boldsymbol{e}_h$ and ε_h for velocity and pressure are defined as follows,

$$\boldsymbol{e}_h = \{\boldsymbol{e}_0,\ \boldsymbol{e}_b\} = Q_h\boldsymbol{u} - \boldsymbol{u}_h = \{Q_0\boldsymbol{u} - \boldsymbol{u}_0,\ Q_b\boldsymbol{u} - \boldsymbol{u}_b\}, \qquad \varepsilon_h = \mathbb{Q}_h p - p_h. \tag{33}$$

For vectors $\boldsymbol{u} = (u_1, u_2)$ and $\boldsymbol{v} = (v_1, v_2)$, we define the following notation,

$$\boldsymbol{u}^T\boldsymbol{v} = \begin{pmatrix} u_1v_1 & u_1v_2 \\ u_2v_1 & u_2v_2 \end{pmatrix}, \quad \nabla\boldsymbol{v} = \begin{pmatrix} \frac{\partial v_1}{\partial x_1} & \frac{\partial v_2}{\partial x_1} \\ \frac{\partial v_1}{\partial x_2} & \frac{\partial v_2}{\partial x_2} \end{pmatrix},$$

and a functional as follows,

$$\begin{aligned}
\ell_{\boldsymbol{u},\boldsymbol{u}_h}(\boldsymbol{v}) = {} & a_{sk}(\boldsymbol{u}, \boldsymbol{u} - Q_0\boldsymbol{u}, \boldsymbol{v}_0) + a_{sk}(\boldsymbol{u} - Q_0\boldsymbol{u}, Q_0\boldsymbol{u}, \boldsymbol{v}_0) \\
& + a_{sk,w}(Q_h\boldsymbol{u}, \boldsymbol{e}_h, \boldsymbol{v}) + a_{sk,w}(\boldsymbol{e}_h, \boldsymbol{u}_h, \boldsymbol{v}) \\
& + \frac{1}{2}\langle \boldsymbol{v}_0 - \boldsymbol{v}_b,\ \mathbf{n}\cdot(\boldsymbol{u}^T\boldsymbol{u})\rangle_{\partial\mathcal{T}_h} + \frac{1}{2}\langle Q_0\boldsymbol{u} - Q_b\boldsymbol{u},\ \mathbf{n}\cdot\mathbf{Q}_h(Q_0\boldsymbol{u}^T\boldsymbol{v}_0)\rangle_{\partial\mathcal{T}_h} \\
& - \frac{1}{2}\langle \boldsymbol{v}_0 - \boldsymbol{v}_b,\ \mathbf{n}\cdot\mathbf{Q}_h(Q_0\boldsymbol{u}^TQ_0\boldsymbol{u})\rangle_{\partial\mathcal{T}_h}.
\end{aligned} \tag{34}$$

Next we show that the functional (34) is the residual for the convection term.

Lemma 4.1. *Let $\ell_{\boldsymbol{u},\boldsymbol{u}_h}(\boldsymbol{v})$ be defined in (34) and $\boldsymbol{e}_h$ be defined in (33), then*

$$(\boldsymbol{u}\cdot\nabla\boldsymbol{u}, \boldsymbol{v}_0)_{\mathcal{T}_h} - a_{sk,w}(\boldsymbol{u}_h, \boldsymbol{u}_h, \boldsymbol{v}) = \ell_{\boldsymbol{u},\boldsymbol{u}_h}(\boldsymbol{v}). \tag{35}$$

Proof. Since $\nabla\cdot\boldsymbol{u} = 0$, the following equation can be verified easily for any $\boldsymbol{v} \in V_h^0$,

$$\begin{aligned}
(\boldsymbol{u}\cdot\nabla\boldsymbol{u}, \boldsymbol{v}_0)_{\mathcal{T}_h} &= a_{sk}(\boldsymbol{u}, \boldsymbol{u}, \boldsymbol{v}_0) + \frac{1}{2}\langle \boldsymbol{u},\ \mathbf{n}\cdot(\boldsymbol{u}^T\boldsymbol{v}_0)\rangle_{\partial\mathcal{T}_h} \\
&= a_{sk}(\boldsymbol{u}, \boldsymbol{u}, \boldsymbol{v}_0) + \frac{1}{2}\langle \boldsymbol{v}_0,\ \mathbf{n}\cdot(\boldsymbol{u}^T\boldsymbol{u})\rangle_{\partial\mathcal{T}_h}, \\
&= a_{sk}(\boldsymbol{u}, \boldsymbol{u}, \boldsymbol{v}_0) + \frac{1}{2}\langle \boldsymbol{v}_0 - \boldsymbol{v}_b,\ \mathbf{n}\cdot(\boldsymbol{u}^T\boldsymbol{u})\rangle_{\partial\mathcal{T}_h}.
\end{aligned} \tag{36}$$

For $\boldsymbol{\sigma} = \{\boldsymbol{\sigma}_0, \boldsymbol{\sigma}_b\}$, $\boldsymbol{v} = \{\boldsymbol{v}_0, \boldsymbol{v}_b\}$ and $\boldsymbol{w} = \{\boldsymbol{w}_0, \boldsymbol{w}_b\}$ in V_h, by the definition of the weak gradient (8), we obtain

$$\begin{aligned}
(\boldsymbol{\sigma}\cdot\nabla_w\boldsymbol{v}, \boldsymbol{w})_T &= (\boldsymbol{\sigma}_0\cdot\nabla_w\boldsymbol{v}, \boldsymbol{w}_0)_T \\
&= (\nabla_w\boldsymbol{v}, \boldsymbol{\sigma}_0^T\boldsymbol{w}_0)_T \\
&= -(\boldsymbol{v}_0, \nabla\cdot\mathbf{Q}_h(\boldsymbol{\sigma}_0^T\boldsymbol{w}_0))_T + \langle \boldsymbol{v}_b,\ \mathbf{n}\cdot\mathbf{Q}_h(\boldsymbol{\sigma}_0^T\boldsymbol{w}_0)\rangle_{\partial T} \\
&= (\boldsymbol{\sigma}_0\cdot\nabla\boldsymbol{v}_0, \boldsymbol{w}_0)_T - \langle \boldsymbol{v}_0 - \boldsymbol{v}_b,\ \mathbf{n}\cdot\mathbf{Q}_h(\boldsymbol{\sigma}_0^T\boldsymbol{w}_0)\rangle_{\partial T}.
\end{aligned}$$

Therefore, we have

$$\begin{aligned}
a_{sk,w}(Q_h\boldsymbol{u}, Q_h\boldsymbol{u}, \boldsymbol{v}) = {} & a_{sk}(Q_0\boldsymbol{u}, Q_0\boldsymbol{u}, \boldsymbol{v}_0) - \frac{1}{2}\langle Q_0\boldsymbol{u} - Q_b\boldsymbol{u},\ \mathbf{n}\cdot\mathbf{Q}_h(Q_0\boldsymbol{u}^T\boldsymbol{v}_0)\rangle_{\partial\mathcal{T}_h} \\
& + \frac{1}{2}\langle \boldsymbol{v}_0 - \boldsymbol{v}_b,\ \mathbf{n}\cdot\mathbf{Q}_h(Q_0\boldsymbol{u}^TQ_0\boldsymbol{u})\rangle_{\partial\mathcal{T}_h}.
\end{aligned} \tag{37}$$

It is easy to see

$$a_{sk}(\boldsymbol{u}, \boldsymbol{u}, \boldsymbol{v}_0) - a_{sk}(Q_0\boldsymbol{u}, Q_0\boldsymbol{u}, \boldsymbol{v}_0) = a_{sk}(\boldsymbol{u}, \boldsymbol{u} - Q_0\boldsymbol{u}, \boldsymbol{v}_0) + a_{sk}(\boldsymbol{u} - Q_0\boldsymbol{u}, Q_0\boldsymbol{u}, \boldsymbol{v}_0) \tag{38}$$

$$a_{sk,w}(Q_h\boldsymbol{u}, Q_h\boldsymbol{u}, \boldsymbol{v}) - a_{sk,w}(\boldsymbol{u}_h, \boldsymbol{u}_h, \boldsymbol{v}) = a_{sk,w}(Q_h\boldsymbol{u}, \boldsymbol{e}_h, \boldsymbol{v}) + a_{sk,w}(\boldsymbol{e}_h, \boldsymbol{u}_h, \boldsymbol{v}). \tag{39}$$

Using (36), (37), (38), and (39), we have

$$\begin{aligned}
(\boldsymbol{u}\cdot\nabla\boldsymbol{u}, \boldsymbol{v}_0)_{\mathcal{T}_h} - a_{sk,w}(\boldsymbol{u}_h, \boldsymbol{u}_h, \boldsymbol{v}) &= (\boldsymbol{u}\cdot\nabla\boldsymbol{u}, \boldsymbol{v}_0)_{\mathcal{T}_h} - a_{sk,w}(Q_h\boldsymbol{u}, Q_h\boldsymbol{u}, \boldsymbol{v})\\
&\quad + a_{sk,w}(Q_h\boldsymbol{u}, Q_h\boldsymbol{u}, \boldsymbol{v}) - a_{sk,w}(\boldsymbol{u}_h, \boldsymbol{u}_h, \boldsymbol{v})\\
&= a_{sk}(\boldsymbol{u}, \boldsymbol{u}, \boldsymbol{v}) - a_{sk}(Q_0\boldsymbol{u}, Q_0\boldsymbol{u}, \boldsymbol{v}_0)\\
&\quad + a_{sk,w}(Q_h\boldsymbol{u}, Q_h\boldsymbol{u}, \boldsymbol{v}) - a_{sk,w}(\boldsymbol{u}_h, \boldsymbol{u}_h, \boldsymbol{v})\\
&\quad + \frac{1}{2}\langle \boldsymbol{v}_0 - \boldsymbol{v}_b,\ \mathbf{n}\cdot(\boldsymbol{u}^T\boldsymbol{u})\rangle_{\partial\mathcal{T}_h}\\
&\quad + \frac{1}{2}\langle Q_0\boldsymbol{u} - Q_b\boldsymbol{u},\ \mathbf{n}\cdot\mathbf{Q}_h(Q_0\boldsymbol{u}^T\boldsymbol{v}_0)\rangle_{\partial\mathcal{T}_h}\\
&\quad - \frac{1}{2}\langle \boldsymbol{v}_0 - \boldsymbol{v}_b,\ \mathbf{n}\cdot\mathbf{Q}_h(Q_0\boldsymbol{u}^T Q_0\boldsymbol{u})\rangle_{\partial\mathcal{T}_h}\\
&= \ell_{\boldsymbol{u},\boldsymbol{u}_h}(\boldsymbol{v}),
\end{aligned}$$

which completes the proof. □

Based on Lemma 4.1, we derive the error equations which are summarized in the following lemma.

Lemma 4.2. *Let $\boldsymbol{e}_h$ and ε_h be defined in (33). Then, we have*

$$a(\boldsymbol{e}_h,\ \boldsymbol{v}) - b(\boldsymbol{v},\ \varepsilon_h) = \varphi_{\boldsymbol{u},p}(\boldsymbol{v}) - \ell_{\boldsymbol{u},\boldsymbol{u}_h}(\boldsymbol{v}), \quad \forall \boldsymbol{v}\in V_h^0 \tag{40}$$

$$b(\boldsymbol{e}_h,\ q) = 0, \qquad \forall q\in W_h, \tag{41}$$

where

$$\begin{aligned}
\varphi_{\boldsymbol{u},p}(\boldsymbol{v}) &= \mu\langle \boldsymbol{v}_0 - \boldsymbol{v}_b, \nabla\boldsymbol{u}\cdot\mathbf{n} - \mathbf{Q}_h(\nabla\boldsymbol{u})\cdot\mathbf{n}\rangle_{\partial\mathcal{T}_h}\\
&\quad + \mu s(Q_h\boldsymbol{u}, \boldsymbol{v}) - \langle \boldsymbol{v}_0 - \boldsymbol{v}_b, (p - \mathbb{Q}_h p)\mathbf{n}\rangle_{\partial\mathcal{T}_h}.
\end{aligned} \tag{42}$$

Proof. Let $\boldsymbol{v} = \{\boldsymbol{v}_0, \boldsymbol{v}_b\}\in V_h^0$. Testing (1) by $\boldsymbol{v}_0$ gives

$$-\mu(\Delta\boldsymbol{u}, \boldsymbol{v}_0) + (\boldsymbol{u}\cdot\nabla\boldsymbol{u}, \boldsymbol{v}_0) + (\nabla p, \boldsymbol{v}_0) = (\mathbf{f}, \boldsymbol{v}_0). \tag{43}$$

The following two equations can be verified easily and also can be found in [26],

$$\begin{aligned}
-\mu(\Delta\boldsymbol{u}, \boldsymbol{v}_0) &= \mu(\nabla_w(Q_h\boldsymbol{u}), \nabla_w\boldsymbol{v})_{\mathcal{T}_h} - \mu\langle \boldsymbol{v}_0 - \boldsymbol{v}_b, (\nabla\boldsymbol{u} - \mathbf{Q}_h(\nabla\boldsymbol{u}))\cdot\mathbf{n}\rangle_{\partial\mathcal{T}_h},\\
(\boldsymbol{v}_0, \nabla p) &= -(\nabla_w\cdot\boldsymbol{v}, \mathbb{Q}_h p)_{\mathcal{T}_h} + \langle \boldsymbol{v}_0 - \boldsymbol{v}_b, (p - \mathbb{Q}_h p)\mathbf{n}\rangle_{\partial\mathcal{T}_h}.
\end{aligned}$$

Then (43) becomes

$$\begin{aligned}
\mu(\nabla_w(Q_h\boldsymbol{u}), \nabla_w\boldsymbol{v})_{\mathcal{T}_h} + (\boldsymbol{u}\cdot\nabla\boldsymbol{u}, \boldsymbol{v}_0) - (\nabla_w\cdot\boldsymbol{v}, \mathbb{Q}_h p) &= (\mathbf{f}, \boldsymbol{v}_0)\\
&\quad + \mu\langle \boldsymbol{v}_0 - \boldsymbol{v}_b, \nabla\boldsymbol{u}\cdot\mathbf{n} - \mathbf{Q}_h(\nabla\boldsymbol{u})\cdot\mathbf{n}\rangle_{\partial\mathcal{T}_h} - \langle \boldsymbol{v}_0 - \boldsymbol{v}_b, (p - \mathbb{Q}_h p)\mathbf{n}\rangle_{\partial\mathcal{T}_h}.
\end{aligned}$$

Adding $\mu s(Q_h\boldsymbol{u}, \boldsymbol{v})$ to the both sides of the above equation, we obtain

$$a_w(Q_h\boldsymbol{u}, \boldsymbol{v}) + (\boldsymbol{u}\cdot\nabla\boldsymbol{u}, \boldsymbol{v}_0) - b_w(\boldsymbol{v}, \mathbb{Q}p) = (\mathbf{f}, \boldsymbol{v}_0) + \varphi_{\boldsymbol{u},p}(\boldsymbol{v}). \tag{44}$$

Subtracting (44) and (10) and applying (35) from Lemma 4.1, we have,

$$\begin{aligned}
a(\boldsymbol{e}_h, \boldsymbol{v}) - b(\boldsymbol{v}, \varepsilon_h) &= \varphi_{\boldsymbol{u},p}(\boldsymbol{v}) - (\boldsymbol{u}\cdot\nabla\boldsymbol{u}, \boldsymbol{v}_0) + a_{sk,w}(\boldsymbol{u}_h, \boldsymbol{u}_h, \boldsymbol{v})\\
&= \varphi_{\boldsymbol{u},p}(\boldsymbol{v}) - \ell_{\boldsymbol{u},\boldsymbol{u}_h}(\boldsymbol{v}),
\end{aligned} \tag{45}$$

which gives (40).

To derive (41), we test (2) by $q\in W_h$ and use (16) to obtain

$$0 = (\nabla\cdot\boldsymbol{u}, q) = (\nabla_w\cdot Q_h\boldsymbol{u}, q). \tag{46}$$

Subtracting (46) and (11) yields (41) which completes the proof. □

Based on the error equations given in Lemma 4.2, we can derive the error estimates naturally. Let K be an element with e as an edge. The following trace inequality is well known, i.e., there exists a constant C such that for any function $g \in H^1(K)$

$$\|g\|_e^2 \le C\left(h_K^{-1}\|g\|_K^2 + h_K\|\nabla g\|_K^2\right). \tag{47}$$

Lemma 4.3. *Let $\ell_{\boldsymbol{u},\boldsymbol{u}_h}(\boldsymbol{v})$ be defined in (34), then,*

$$\ell_{\boldsymbol{u},\boldsymbol{u}_h}(\boldsymbol{e}_h) \le Ch^k\|\boldsymbol{u}\|_{k+1}^2 |||\boldsymbol{e}_h||| + \frac{\mathcal{N}_h\|\mathbf{f}\|_{*,h}}{\mu}|||\boldsymbol{e}_h|||^2. \tag{48}$$

Proof. Since $a_{sk,w}(Q_0\boldsymbol{u}, \boldsymbol{e}_h, \boldsymbol{e}_h) = 0$, we have

$$\begin{aligned}\ell_{\boldsymbol{u},\boldsymbol{u}_h}(\boldsymbol{e}_h) &= a_{sk}(\boldsymbol{u}, \boldsymbol{u} - Q_0\boldsymbol{u}, \boldsymbol{e}_0) + a_{sk}(\boldsymbol{u} - Q_0\boldsymbol{u}, Q_0\boldsymbol{u}, \boldsymbol{e}_0)\\ &\quad + a_{sk,w}(\boldsymbol{e}_h, \boldsymbol{u}_h, \boldsymbol{e}_h) + \frac{1}{2}\langle \boldsymbol{e}_0 - \boldsymbol{e}_b,\ \mathbf{n}\cdot(\boldsymbol{u}^T\boldsymbol{u})\rangle_{\partial\mathcal{T}_h}\\ &\quad + \frac{1}{2}\langle Q_0\boldsymbol{u} - Q_b\boldsymbol{u},\ \mathbf{n}\cdot\mathbf{Q}_h(Q_0\boldsymbol{u}^T\boldsymbol{e}_0)\rangle_{\partial\mathcal{T}_h} - \frac{1}{2}\langle \boldsymbol{e}_0 - \boldsymbol{e}_b,\ \mathbf{n}\cdot\mathbf{Q}_h(Q_0\boldsymbol{u}^TQ_0\boldsymbol{u})\rangle_{\partial\mathcal{T}_h}.\end{aligned}$$

Next we will estimate all the terms on the right hand side one by one. For the first term, it follows from (23), (21) and the definition of Q_0 that

$$|a_{sk}(\boldsymbol{u}, \boldsymbol{u} - Q_0\boldsymbol{u}, \boldsymbol{e}_0)| \le C|||\boldsymbol{u}|||_1 |||\boldsymbol{u} - Q_0\boldsymbol{u}|||_1 |||\boldsymbol{e}|||_1 \le Ch^k\|\boldsymbol{u}\|_1\|\boldsymbol{u}\|_{k+1}|||\boldsymbol{e}|||.$$

Similarly, we have the following estimate for the second term,

$$|a_{sk}(\boldsymbol{u} - Q_0\boldsymbol{u}, Q_0\boldsymbol{u}, \boldsymbol{e}_0)| \le Ch^k\|\boldsymbol{u}\|_1\|\boldsymbol{u}\|_{k+1}|||\boldsymbol{e}|||.$$

For the third term, (24) and (30) imply

$$|a_{sk,w}(\boldsymbol{e}_h, \boldsymbol{u}_h, \boldsymbol{e}_h)| \le \mathcal{N}_h|||\boldsymbol{u}_h||| \, |||\boldsymbol{e}_h|||^2 \le \mathcal{N}_h\frac{\|\mathbf{f}\|_{*,h}}{\mu}|||\boldsymbol{e}_h|||^2.$$

Using the trace inequality (47), inverse inequality, (22) and (21), we have the following estimate for the fifth term,

$$\begin{aligned}\frac{1}{2}\langle Q_0\boldsymbol{u} - Q_b\boldsymbol{u},\ \mathbf{n}\cdot\mathbf{Q}_h(Q_0\boldsymbol{u}^T\boldsymbol{e}_0)\rangle_{\partial\mathcal{T}_h} &\le \frac{1}{2}\Big(\sum_{T\in\mathcal{T}_h} h^{-1}\|Q_0\boldsymbol{u} - \boldsymbol{u}\|_{\partial T}^2\Big)^{1/2}\Big(\sum_{T\in\mathcal{T}_h} h\|\mathbf{Q}_h(Q_0\boldsymbol{u}^T\boldsymbol{e}_0)\|_{\partial T}^2\Big)^{1/2}\\ &\le Ch^k\|\boldsymbol{u}\|_{k+1}\Big(\sum_{T\in\mathcal{T}_h}\|Q_0\boldsymbol{u}^T\boldsymbol{e}_0\|_T^2\Big)^{1/2}\\ &\le Ch^k\|\boldsymbol{u}\|_{k+1}\|Q_0\boldsymbol{u}\|_{L^4(\Omega)}\|\boldsymbol{e}_0\|_{L^4(\Omega)}\\ &\le Ch^k\|\boldsymbol{u}\|_{k+1}\|\boldsymbol{u}\|_1|||\boldsymbol{e}_h|||\\ &\le Ch^k\|\boldsymbol{u}\|_1\|\boldsymbol{u}\|_{k+1}|||\boldsymbol{e}_h|||.\end{aligned}$$

For the third and last term, we estimate them together using similar techniques based on the trace inequality (47), inverse inequality, (22) and (21) and obtain,

$$\begin{aligned}&\frac{1}{2}\sum_{T\in\mathcal{T}_h}\big(\langle \boldsymbol{e}_0 - \boldsymbol{e}_b,\ \mathbf{n}\cdot(\boldsymbol{u}^T\boldsymbol{u})\rangle_{\partial T} - \langle \boldsymbol{e}_0 - \boldsymbol{e}_b,\ \mathbf{n}\cdot\mathbf{Q}_h(Q_0\boldsymbol{u}^TQ_0\boldsymbol{u})\rangle_{\partial T}\big)\\ &= \frac{1}{2}\sum_{T\in\mathcal{T}_h}\big(\langle \boldsymbol{e}_0 - \boldsymbol{e}_b,\ \mathbf{n}\cdot(\boldsymbol{u}^T\boldsymbol{u} - \mathbf{Q}_h\boldsymbol{u}^T\boldsymbol{u})\rangle_{\partial T} - \langle \boldsymbol{e}_0 - \boldsymbol{e}_b,\ \mathbf{n}\cdot\mathbf{Q}_h(Q_0\boldsymbol{u}^TQ_0\boldsymbol{u} - \boldsymbol{u}^T\boldsymbol{u})\rangle_{\partial T}\big)\\ &\le C\left[\left(\sum_{T\in\mathcal{T}_h} h_T^{-1}\|\boldsymbol{e}_0 - \boldsymbol{e}_b\|_{\partial T}^2\right)^{1/2}\left(\sum_{T\in\mathcal{T}_h} h_T\|\boldsymbol{u}^T\boldsymbol{u} - \mathbf{Q}_h\boldsymbol{u}^T\boldsymbol{u}\|_{\partial T}^2\right)^{1/2}\right.\\ &\quad\left. + \left(\sum_{T\in\mathcal{T}_h} h_T^{-1}\|\boldsymbol{e}_0 - \boldsymbol{e}_b\|_{\partial T}^2\right)^{1/2}\left(\sum_{T\in\mathcal{T}_h} h_T\|\mathbf{Q}_h(Q_0\boldsymbol{u}^TQ_0\boldsymbol{u} - \boldsymbol{u}^T\boldsymbol{u})\|_{\partial T}^2\right)^{1/2}\right]\\ &\le C|||\boldsymbol{e}_h|||\left[\left(\sum_{T\in\mathcal{T}_h}(\|\boldsymbol{u}^T\boldsymbol{u} - \mathbf{Q}_h\boldsymbol{u}^T\boldsymbol{u}\|_T^2 + h_T^2\|\nabla(\boldsymbol{u}^T\boldsymbol{u} - \mathbf{Q}_h\boldsymbol{u}^T\boldsymbol{u})\|_T^2)\right)^{1/2}\right.\end{aligned}$$

$$
\begin{aligned}
&+\left.\left(\sum_{T\in\mathcal{T}_h}\|\mathbb{Q}_0\boldsymbol{u}^T\mathbb{Q}_0\boldsymbol{u}-\boldsymbol{u}^T\boldsymbol{u}\|_T^2\right)^{1/2}\right]\\
&\le Ch^k(\|\boldsymbol{u}^T\boldsymbol{u}\|_k+\|\boldsymbol{u}\|_{k+1}^2)|||\boldsymbol{e}_h|||\\
&\le Ch^k\|\boldsymbol{u}\|_{k+1}^2|||\boldsymbol{e}_h|||.
\end{aligned}
$$

Then (48) follows by combining all the estimates. □

The estimate for $\varphi_{\boldsymbol{u},p}(\boldsymbol{e}_h)$ has been proved in [26] and we only present the results here in the following lemma without the proof.

Lemma 4.4. *Let $\varphi_{\boldsymbol{u},p}(\boldsymbol{v})$ be defined in (34), then,*

$$
\varphi_{\boldsymbol{u},p}(\boldsymbol{e}_h)\le Ch^k(\|\boldsymbol{u}\|_{k+1}+\|p\|_k)|||\boldsymbol{e}_h|||. \tag{49}
$$

Now, combining all the estimates in Lemmas 4.3 and 4.4, we have the following overall error estimates of the WG scheme (10)–(11).

Theorem 3. *Let $(\boldsymbol{u},p)\in[H_0^1(\Omega)\cap H^{k+1}(\Omega)]^d\times(L_0^2(\Omega)\cap H^k(\Omega))$, $k\ge 1$, and $(\boldsymbol{u}_h,p_h)\in V_h\times W_h$ be the solution of (1)– (3) and (10)– (11), respectively. If $\rho\equiv\frac{\mathcal{N}_h\|\mathbf{f}\|_{*,h}}{\mu^2}<1$, then the following error estimate holds*

$$
|||\mathbb{Q}_h\boldsymbol{u}-\boldsymbol{u}_h|||+\|\mathbb{Q}_hp-p_h\|\le Ch^k(\|\boldsymbol{u}\|_{k+1}+\|p\|_k). \tag{50}
$$

Proof. By letting $\boldsymbol{v}=\boldsymbol{e}_h$ in (40) and $q=\varepsilon_h$ in (41) and adding the two resulting equations, we have

$$
\mu|||\boldsymbol{e}_h|||^2=\varphi_{\boldsymbol{u},p}(\boldsymbol{e}_h)-\ell_{\boldsymbol{u},\boldsymbol{u}_h}(\boldsymbol{e}_h). \tag{51}
$$

It then follows from (49) and (48) that

$$
\mu|||\boldsymbol{e}_h|||^2\le Ch^k(\|\boldsymbol{u}\|_{k+1}+\|p\|_k)|||\boldsymbol{e}_h|||+\mathcal{N}_h\frac{\|\mathbf{f}\|_{*,h}}{\mu}|||\boldsymbol{e}_h|||^2, \tag{52}
$$

which implies the first part of (50). To estimate $\|\varepsilon_h\|$, from (40), we have that

$$
b(\boldsymbol{v},\varepsilon_h)=a(\boldsymbol{e}_h,\boldsymbol{v})-\varphi_{\boldsymbol{u},p}(\boldsymbol{v})+\ell_{\boldsymbol{u},\boldsymbol{u}_h}(\boldsymbol{v}).
$$

Then by (13), (52), (49), and (48), we have

$$
|b(\boldsymbol{v},\varepsilon_h)|\le Ch^k(\|\boldsymbol{u}\|_{k+1}+\|p\|_k)|||\boldsymbol{v}|||.
$$

Applying the inf–sup condition (17) gives

$$
\|\varepsilon_h\|\le Ch^k(\|\boldsymbol{u}\|_{k+1}+\|p\|_k),
$$

which yields the estimate (50) and completes the proof. □

5. Numerical experiment

In this section, we present some numerical results to demonstrate the effectiveness of our proposed WG scheme for solving the NS equations. In all the numerical experiments, we use Newton's method to linearize the nonlinear discrete problem.

5.1. Example 1

Let $\Omega=(0,1)^2$ and the load term $\mathbf{f}$ be chosen such that the analytical solution is

$$
\boldsymbol{u}(x,y)=\frac{1}{2}\begin{pmatrix}\sin(2\pi x)^2\sin(2\pi y)\cos(2\pi y)\\-\sin(2\pi y)^2\sin(2\pi x)\cos(2\pi x)\end{pmatrix},
$$

and

$$
p(x,y)=\pi^2\sin(2\pi x)\cos(2\pi y).
$$

In this test, we assume $\mu=1$. The Weak Galerkin algorithm (10)–(11) is performed on the polygonal mesh and rectangular mesh, which are shown in Fig. 1.

The error profiles and convergence results are reported in Table 1. Here, $k=1$, i.e., the linear WG elements are used. From the table, we observe that the H^1-error for velocity and L^2-error for pressure converge at the order $\mathcal{O}(h)$ which confirm our theoretical results (50). Moreover, the L^2-norm for velocity has the convergence rate $\mathcal{O}(h^2)$ as expected.

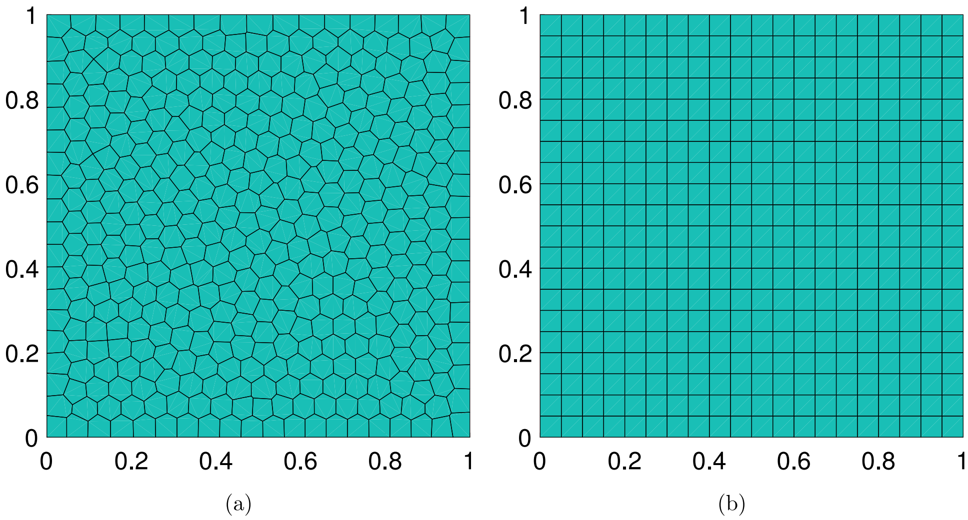

Fig. 1. (a) Polygonal mesh with $h = 1/20$; (b) Uniform rectangular mesh with $h = 1/20$.

Table 1
Example 1: the errors and convergence rates for $k = 1$.

$1/h$	$\\|\mathbf{u}_h - Q_h\mathbf{u}\\|$	Rate	$\\|\mathbf{u}_0 - Q_0\mathbf{u}\\|$	Rate	$\\|p_h - \mathbb{Q}_h p\\|$	Rate
Polygonal mesh						
10	2.6018E+00		1.5376E−01		1.4033E+00	
20	1.3016E+00	9.99E−01	4.1775E−02	1.88E+00	3.2400E−01	2.11E+00
40	6.4198E−01	1.02E+00	1.0443E−02	2.00E+00	9.2675E−02	1.81E+00
80	3.2166E−01	9.97E−01	2.6264E−03	1.99E+00	4.7188E−02	9.74E−01
160	1.6009E−01	1.01E+00	6.5519E−04	2.00E+00	2.3594E−02	1.00E+00
Rectangular mesh						
10	3.1723E+00		2.0289E−01		9.2295E−01	
20	1.6961E+00	9.03E−01	5.8146E−02	1.80E+00	7.9796E−01	2.10E−01
40	8.6848E−01	9.66E−01	1.5322E−02	1.92E+00	1.1864E−01	2.75E+00
80	4.3746E−01	9.89E−01	3.8972E−03	1.98E+00	5.9356E−02	9.99E−01
160	2.1873E−01	1.00E+00	9.7430E−04	2.00E+00	2.9678E−02	1.00E+00

Table 2
Example 2: the errors and convergence rates for $k = 1$.

$1/h$	$\\|\mathbf{u}_h - Q_h\mathbf{u}\\|$	Rate	$\\|\mathbf{u}_0 - Q_0\mathbf{u}\\|$	Rate	$\\|p_h - \mathbb{Q}_h p\\|$	Rate
Polygonal mesh						
10	3.9665E−02		2.3218E−03		2.1753e−02	
20	2.0759E−02	9.34E−01	6.4369E−04	1.85E+00	9.3476e−03	1.22E+00
40	1.0955E−02	9.22E−01	1.7918E−04	1.85E+00	3.3874e−03	1.46E+00
80	5.2472E−03	1.06E+00	4.1171E−05	2.12E+00	9.8165e−04	1.79E+00
160	2.5867E−03	1.02E+00	9.9757E−06	2.05E+00	2.8741e−04	1.77E+00
Rectangular mesh						
10	4.4196e−02		2.9201e−03		2.5723e−02	
20	2.3848e−02	8.90E−01	8.6110e−04	1.76E+00	1.3383e−02	9.43E−01
40	1.2396e−02	9.44E−01	2.3433e−04	1.88E+00	4.4252e−03	1.60E+00
80	6.3004e−03	9.76E−01	6.0742e−05	1.95E+00	1.3712e−03	1.69E+00
160	3.0502e−03	1.05E+00	1.4186e−05	2.10E+00	3.8089e−04	1.85E+00

5.2. Example 2

Let $\Omega = (0, 1)^2$ and the load term $\mathbf{f}$ be chosen such that the analytical solution is

$$\mathbf{u}(x, y) = \begin{pmatrix} 0.1x^2(1-x)^2(4y^3 - 6y^2 + 2y) \\ 0.1y^2(1-y)^2(4x^3 - 6x^2 + 2x) \end{pmatrix}$$

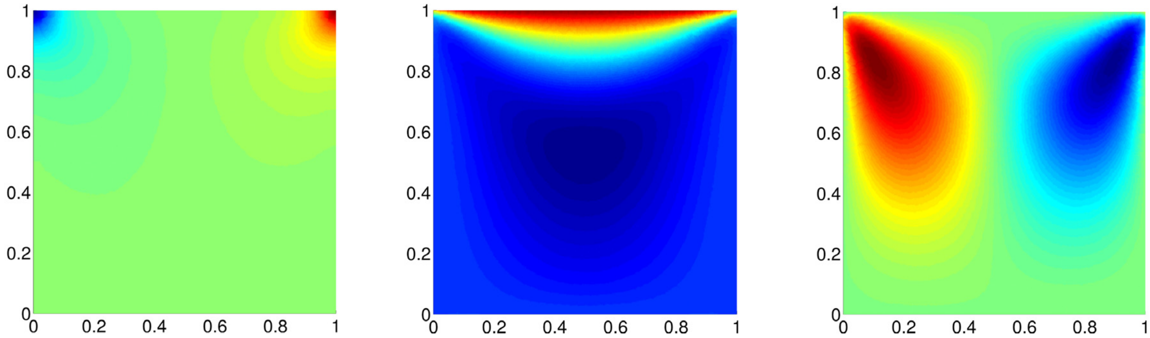

Fig. 2. Example 3: plots of numerical solutions with $\mu = 1$ on the polygonal mesh with $h = 1/40$; pressure p_h (left), x-component of $\boldsymbol{u}_h$ (middle), and y-component of $\boldsymbol{u}_h$ (right).

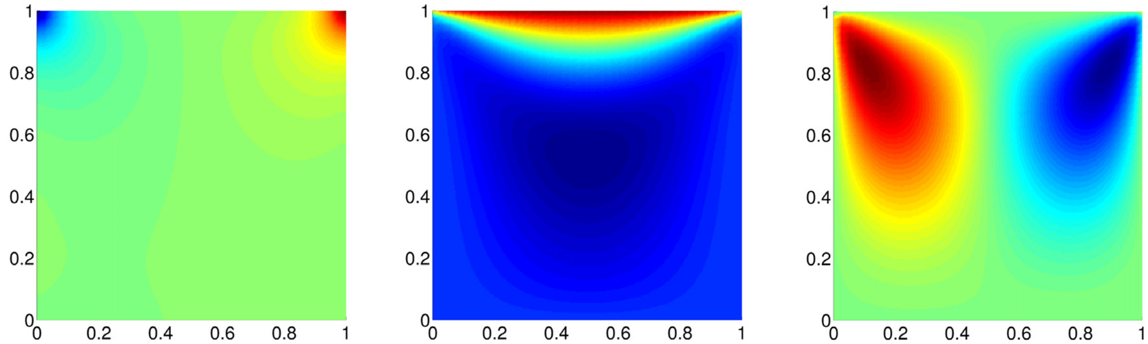

Fig. 3. Example 3: Plots of numerical solutions with $\mu = 1$ on the rectangular mesh with $h = 1/40$; pressure p_h (left), x-component of $\boldsymbol{u}_h$ (middle), and y-component of $\boldsymbol{u}_h$ (right).

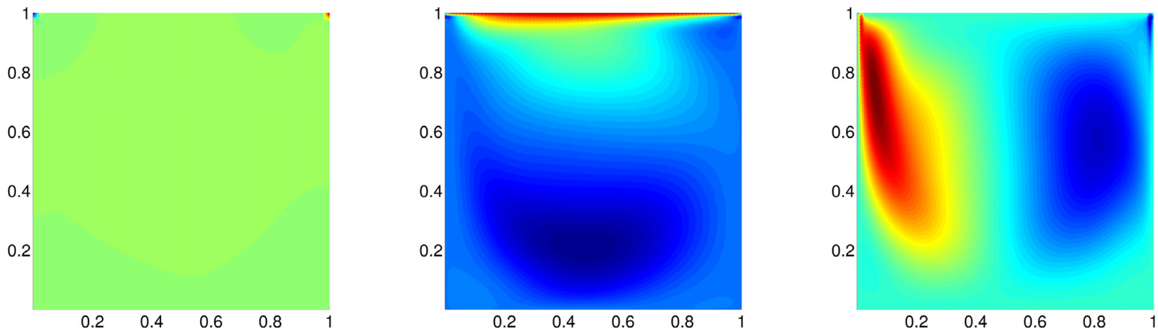

Fig. 4. Example 3: plots of numerical solutions with $\mu = 1\text{E}-3$ on the rectangular mesh with $h = 1/80$; pressure p_h (left), x-component of $\boldsymbol{u}_h$ (middle), and y-component of $\boldsymbol{u}_h$ (right).

and

$$p(x, y) = x^3y^3 - 1/16.$$

Note that in this test the velocity $\boldsymbol{u}$ is not divergence free, i.e., $\nabla \cdot \boldsymbol{u} = g \neq 0$. Therefore, in the WG approximation, the right-hand side in (11) is modified from 0 to $(g, q)^T$.

Again, we choose $\mu = 1$ and $k = 1$ in this example. The numerical tests are conducted on polygonal mesh and rectangular mesh, which are shown in Fig. 1.

The error profiles are reported in Table 2. The convergence results for velocity and pressure confirm our theoretical conclusions (50). Furthermore, superconvergence of pressure measured in L^2-error can be observed.

5.3. Example 3

Let $\Omega = (0, 1)^2$. A lid-driven cavity flow is considered in this test. Set $\mathbf{f} = 0$ and the Dirichlet boundary condition is given as,

$$u|_{\partial\Omega} = \mathbf{g} = \begin{cases} (1, 0)^T, & \text{if } y = 1, \\ (0, 0)^T, & \text{else.} \end{cases}$$

Both polygonal mesh and rectangular mesh with $h = 1/40$ are used in the experiment. Here, we choose $\mu = 1$. The numerical solutions are plotted in Figs. 2–4 for pressure and the components of velocity, respectively.

References

[1] R. Teman, Navier-Stokes Equations: Theory and Numerical Analysis, North-Holland Publishing Company, 1977.
[2] F. Brezzi, On the Existence, Uniqueness and Approximation of Saddle-point Problems arising from Lagrangian Multipliers, Rev. Franç. Autom. Inf. Rech. Opér. Sér. Rouge 8 (R-2) (1974) 129–151.
[3] D. Boffi, F. Brezzi, M. Fortin, Mixed Finite Element Methods and Applications, Springer, 2013.
[4] V. Girault, P. Raviart, Finite Element Approximation of the Navier-Stokes Equations, Vol. 749, Berlin Springer Verlag, 1979.
[5] V. Girault, P. Raviart, Finite Element Methods for Navier-Stokes Equations: Theory and Algorithms, Vol. 87, Springer Verlag, 1986.
[6] I. Babuška, M. Zlámal, Nonconforming elements in the finite element method with penalty, SIAM J. Numer. Anal. 10 (5) (1973) 863–875.
[7] B. Cockburn, G.E. Karniadakis, C.-W. Shu, The development of discontinuous galerkin methods, in: Discontinuous Galerkin Methods, Springer, 2000, pp. 3–50.
[8] D.N. Arnold, F. Brezzi, B. Cockburn, L.D. Marini, Unified analysis of discontinuous galerkin methods for elliptic problems, SIAM J. Numer. Anal. 39 (5) (2001) 1749–1779, http://dx.doi.org/10.1137/S0036142901384162. URL http://portal.acm.org/ft_gateway.cfm?id=588544{&}type=external{&}coll=Portal{&}dl=GUIDE{&}CFID=80879112{&}CFTOKEN=15019332.
[9] F. Bassi, S. Rebay, A high-order accurate discontinuous finite element method for the numerical solution of the compressible Navier–Stokes equations, J. Comput. Phys. 131 (2) (1997) 267–279.
[10] B. Cockburn, C.W. Shu, The Runge–Kutta discontinuous galerkin method for conservation laws V: Multidimensional systems, J. Comput. Phys. 141 (2) (1998) 199–224.
[11] I. Lomtev, G.E. Karniadakis, A discontinuous Galerkin method for the Navier–Stokes equations, Internat. J. Numer. Methods Fluids 29 (5) (1999) 587–603.
[12] C.M. Klaij, J.J. van der Vegt, H. van der Ven, Space–time discontinuous Galerkin method for the compressible Navier–Stokes equations, J. Comput. Phys. 217 (2) (2006) 589–611.
[13] B. Cockburn, G. Kanschat, D. Schötzau, A note on discontinuous Galerkin divergence-free solutions of the Navier–Stokes equations, J. Sci. Comput. 31 (1) (2007) 61–73.
[14] P.-O. Persson, J. Bonet, J. Peraire, Discontinuous Galerkin Solution of the Navier–Stokes equations on deformable domains, Comput. Methods Appl. Mech. Engrg. 198 (17) (2009) 1585–1595.
[15] L. Beirao da Veiga, F. Brezzi, L. Marini, A. Russo, Virtual element method for general second-order elliptic problems on polygonal meshes, Math. Models Methods Appl. Sci. 26 (04) (2016) 729–750.
[16] L. Beirao da Veiga, F. Brezzi, A. Cangiani, G. Manzini, L.D. Marini, A. Russo, Basic principles of virtual element methods, Math. Models Methods Appl. Sci. 23 (01) (2013) 199–214.
[17] L.B. da Veiga, K. Lipnikov, G. Manzini, The mimetic Finite Difference Method for Elliptic Problems, Vol. 11, Springer, 2014.
[18] D.A. Di Pietro, A. Ern, Hybrid high-order methods for variable-diffusion problems on general meshes, C. R. Math. 353 (1) (2015) 31–34.
[19] D.A. Di Pietro, J. Droniou, A. Ern, A Discontinuous-skeletal Method for Advection-diffusion-reaction on General Meshes, SIAM J. Numer. Anal. 53 (5) (2015) 2135–2157.
[20] N.C. Nguyen, J. Peraire, B. Cockburn, An implicit high-order hybridizable discontinuous Galerkin method for the incompressible Navier–Stokes equations, J. Comput. Phys. 230 (4) (2011) 1147–1170.
[21] W. Qiu, K. Shi, A superconvergent HDG method for the incompressible Navier–Stokes equations on general polyhedral meshes, IMA J. Numer. Anal. 36 (4) (2016) 1943–1967.
[22] L.B. da Veiga, C. Lovadina, G. Vacca, Virtual elements for the Navier-Stokes problem on polygonal meshes, arXiv preprint arXiv:1703.00437, 2017.
[23] J. Wang, X. Ye, A weak Galerkin finite element method for second-order elliptic problems, J. Comput. Appl. Math. 241 (2013) 103–115.
[24] J. Wang, X. Ye, A weak galerkin mixed finite element method for second order elliptic problems, Math. Comp. 83 (289) (2014) 2101–2126.
[25] L. Mu, J. Wang, X. Ye, Weak Galerkin finite element methods on polytopal meshes, Int. J. Numer. Anal. Model. 12 (1) (2015).
[26] J. Wang, X. Ye, A weak Galerkin finite element method for the Stokes equations, Adv. Comput. Math. 42 (1) (2016) 155–174.
[27] L. Mu, X. Wang, X. Ye, A modified weak Galerkin finite element method for the Stokes equations, J. Comput. Appl. Math. 275 (2015) 79–90.
[28] L. Mu, J. Wang, X. Ye, A stable numerical algorithm for the Brinkman equations by weak Galerkin finite element methods, J. Comput. Phys. 273 (2014) 327–342.
[29] C. Wang, J. Wang, R. Wang, R. Zhang, A Locking-free weak Galerkin finite element method for elasticity problems in the primal formulation, J. Comput. Appl. Math. (2015).
[30] X. Hu, L. Mu, X. Ye, Weak Galerkin Method for the Biot's Consolidation Model, Comput. Math. Appl. (2017), http://dx.doi.org/10.1016/j.camwa.2017.07.013. URL http://www.sciencedirect.com/science/article/pii/S0898122117304303.
[31] L. Mu, J. Wang, X. Ye, A weak Galerkin finite element method with polynomial reduction, J. Comput. Appl. Math. 285 (2015) 45–58.
[32] L. Mu, J. Wang, X. Ye, A weak Galerkin method for the reissner–mindlin plate in primary form, J. Sci. Comput. (2017) 1–21.
[33] J. Wang, X. Wang, X. Ye, Finite element methods for the Navier-Stokes equations by H(div) elements, J. Comput. Math. (2008) 410–436.